

This is the peer reviewed version of the following article:

Human dental pulp stem cells expressing STRO-1, c-kit and CD34 markers in peripheral nerve regeneration / Carnevale, Gianluca; Pisciotta, Alessandra; Riccio, Massimo; Bertoni, Laura; De Biasi, Sara; Gibellini, Lara; Zordani, Alessio; Cavallini, Gian Maria; La Sala, Giovanni Battista; Bruzzesi, Giacomo; Ferrari, Adriano; Cossarizza, Andrea; De Pol, Anto. - In: JOURNAL OF TISSUE ENGINEERING AND REGENERATIVE MEDICINE. - ISSN 1932-6254. - 12:2(2018), pp. e774-e785. [10.1002/term.2378]

*Terms of use:*

The terms and conditions for the reuse of this version of the manuscript are specified in the publishing policy. For all terms of use and more information see the publisher's website.

19/12/2025 00:26

# Human dental pulp stem cells expressing STRO-1, c-Kit and CD34 markers in peripheral nerve regeneration

Gianluca Carnevale<sup>1\*</sup>, Alessandra Pisciotta<sup>1</sup>, Massimo Riccio<sup>1</sup>, Laura Bertoni<sup>1</sup>, Sara De Biasi<sup>1</sup>, Lara Gibellini<sup>1</sup>, Alessio Zordani<sup>1</sup>, Gian Maria Cavallini<sup>1</sup>, Giovanni Battista La Sala<sup>2</sup>, Giacomo Bruzzesi<sup>3</sup>, Adriano Ferrari<sup>1,4</sup>, Andrea Cossarizza<sup>1</sup>, Anto de Pol<sup>1</sup>.

<sup>1</sup>*Department of Surgery, Medicine, Dentistry and Morphological Sciences with interest in Transplant, Oncology and Regenerative Medicine, University of Modena and Reggio Emilia, Modena, Italy;*

<sup>2</sup>*Department of Obstetrics and Gynecology, Arcispedale Santa Maria Nuova, Reggio Emilia, Italy;*

<sup>3</sup>*Oro-Maxillo-Facial Department, AUSL Baggiovara, Baggiovara, Modena, Italy*

<sup>4</sup>*Children Rehabilitation Special Unit, IRCCS Arcispedale Santa Maria Nuova, Reggio Emilia, Italy*

\* Corresponding Author: Dr. Gianluca Carnevale PhD,

e-mail: gianluca.carnevale@unimore.it

phone: +39 059 4224828

fax: +39 059 4224859

This article has been accepted for publication and undergone full peer review but has not been through the copyediting, typesetting, pagination and proofreading process which may lead to differences between this version and the Version of Record. Please cite this article as doi: 10.1002/term.2378

## Abstract

Peripheral nerve injuries are a commonly encountered clinical problem and often result in long-term functional defects. The application of stem cells able to differentiate in Schwann cells-like cells *in vitro* and *in vivo*, could represent an attractive therapeutic approach for the treatment of nerve injuries. Further, stem cells sources sharing the same embryological origin of Schwann cells might be considered a suitable tool. The aim of this study was to demonstrate the ability of a neuroectodermal subpopulation of human STRO-1<sup>+</sup>/c-Kit<sup>+</sup>/CD34<sup>+</sup> DPSCs, expressing P75<sup>NTR</sup>, Nestin and SOX-10, to differentiate into Schwann cells-like cells *in vitro* and to promote axonal regeneration *in vivo*, which led to functional recovery as measured by sustained gait improvement, in animal rat model of peripheral nerve injury. Transplanted hDPSCs engrafted into sciatic nerve defect, as revealed by the positive staining against human nuclei, showed the expression of typical Schwann cells markers, S100b and, noteworthy, a significant number of myelinated axons was detected. Moreover, hDPSCs promoted axonal regeneration from proximal to distal stumps one month after transplantation. This study demonstrates that STRO-1<sup>+</sup>/c-Kit<sup>+</sup>/CD34<sup>+</sup> hDPSCs, associated to neural crest derivation, represent a promising source of stem cells for the treatment of demyelinating disorders and might provide a valid alternative tool for future clinical applications to achieve functional recovery after injury or peripheral neuropathies besides minimizing ethical issues.

**Keywords:** human DPSCs, Nestin, ectomesenchyme, neural crest, peripheral nerve regeneration, remyelination, collagen scaffold, STRO-1<sup>+</sup>/c-Kit<sup>+</sup>/CD34<sup>+</sup>

## 1. Introduction

Peripheral nerve injuries are commonly encountered clinical problems and often result in long-term functional defects. Despite early diagnosis and modern surgical techniques to induce an accurate nerve repair, the functional recovery rarely reaches the pre-injury levels. To solve these problematic grafts, many studies evaluated Schwann cells (SCs) in animal models of sciatic nerve injury, demonstrating promotion of axonal regeneration and good functional recovery (Aguayo *et al.*, 1977; Ansselin *et al.*, 1997; Mosahebi *et al.*, 2001). Although SCs play a pivotal role in nerve regeneration, their clinical application is limited for several reasons. One hurdle is for the potential use of SCs for autologous transplantation is feasibility because autologous SCs will not be available immediately after a nerve lesion (Morrissey *et al.*, 1991; Calderón-Martínez *et al.*, 2002). In addition to that, one or more functioning nerves must be sacrificed for the SCs isolation, with the consequence of loss of sensation, neuroma formation and potential donor site morbidity. Furthermore, it is difficult to obtain a sufficient number of cells due to their low proliferative rate, poor survival when grafted into the injured site (Iwashita *et al.*, 2000; Hill *et al.*, 2006). For these reasons the use of stem cells, capable of differentiating into myelinated cells of the peripheral nervous system, represent an alternative therapeutic approach for the treatment of nerve injuries. Particularly, optimal transplantable stem cells are supposed to be easily accessible, capable of rapid expansion in culture as well as full integration into host tissue. To this regard, human mesenchymal stem cells (MSCs) isolated from bone marrow (Mimura *et al.*, 2004), adipose tissue (Liu *et al.*, 2011) amniotic fluid (Pan *et al.*, 2006) and Wharton's jelly of the umbilical cord (Ribeiro *et al.*, 2013) have demonstrated a promising role in peripheral nerve regeneration in experimental animal models, showing capability to differentiate into neural cells. The obvious attraction of these cells is that they are a readily available and are less associated with ethical and legal considerations that complicate the use of other cell sources,

like embryonic- stem cells. Considering the outline of the SCs lineage and their origin from the neural crest during the embryological development (Jessen and Mirsky, 2005), cells that share the same embryological origin, with molecular and phenotypic properties similar to SCs, could be an effective alternative. Human dental pulp stem cells (hDPSCs) could represent a promising alternative source. In fact it is well established that neural crest derived multipotent stem cells migrate to and remain entrapped within the dental pulp, in the early head and during the formation of ectomesenchymal tissue (Caton and Tucker, 2009; Miletich and Sharpe, 2004). As previously described, these ectoderm-derived stem cells originating from migrating neural crest cells not only possess MSCs properties, due to their ability to differentiate into cells of mesodermal lineages, but also have the potential to differentiate along the neural lineage (Miletich and Sharpe, 2004; Chai *et al.*, 2000; Graham *et al.*, 2004; Thesleff and Aberg, 1999). Previous reports from Laino *et al.* (Laino *et al.*, 2005; Laino *et al.*, 2006) and our group (Pisciotta *et al.*, 2015a) demonstrated that a niche of hDPSCs positively sorted for the markers STRO-1, c-Kit and CD34, was able to differentiate towards osteogenic, adipogenic and myogenic lineages, although it could be also differentiated toward neural cytotypes. These hDPSCs expressing STRO-1, c-Kit and CD34 are attributable to a niche of neural crest derivation and indeed are positive for P75<sup>NTR</sup>, also known as CD271, and Nestin. This subpopulation owns many clinical advantages, such as easy accessibility, rapid proliferation *in vitro* and successful integration into the host tissue, thus making them excellent candidates for regenerative medicine purposes, especially in the field of neural tissue engineering (Martens *et al.*, 2013; Gronthos *et al.*, 2002; Ibarretxe *et al.*, 2012; Deng *et al.*, 2001). Although several groups have already reported neuronal differentiation of hDPSCs *in vitro* (Gronthos *et al.*, 2002; Arthur *et al.*, 2008; Kiraly *et al.*, 2009), the differentiation towards SCs has been demonstrated *in vitro* by Martens *et al.* and Al-zer *et al.* (Martens *et al.*, 2014; Al-Zer *et al.*, 2015), on unsorted dental pulp stem cells populations. The goal of this

study was to demonstrate the ability of hDPSCs positively immune-selected for STRO-1, c-Kit and CD34 to differentiate into Schwann cells-like cells when cultured in appropriate medium *in vitro*. Subsequently, we evaluated the ability of transplanted immune-selected hDPSCs to integrate and contribute to healing in rat sciatic nerve injury.

## **2. Materials and methods**

### **2.1. Isolation and culture of hDPSCs**

Human DPSCs were isolated from third molars of adult subjects (21 to 35 years of age, n=5) after informed consent of the patients. Dental pulp was processed and subsequently immune-selected by magnetic cell sorting to obtain the STRO-1<sup>+</sup>/c-Kit<sup>+</sup>/CD34<sup>+</sup> population. Further description of cell isolation and immune-selection procedures is provided in Supplementary information.

### **2.2. *In vitro* multi-lineage differentiation, neural crest markers expression and FACS analysis**

The ability of STRO-1<sup>+</sup>/c-Kit<sup>+</sup>/CD34<sup>+</sup> hDPSCs to differentiate towards osteogenic, adipogenic, myogenic and neurogenic lineages was evaluated culturing the cells in the appropriate induction media as previously described (Pisciotta *et al.*, 2012; Carnevale *et al.*, 2013; Pisciotta *et al.*, 2015a). The expression of P75<sup>NTR</sup>, Nestin and Sox-10 was evaluated through immunofluorescence labelling and FACS analysis on undifferentiated hDPSCs at passage 1. Further details are provided in supplementary information.

## 2.4. Differentiation of hDPSCs into Schwann cells-like-cells phenotype and neurotrophic factors quantification

Human DPSCs were induced to differentiate into Schwann cells-like cells according to a protocol from Dezawa et al. after minor edits (Dezawa *et al.*, 2001). Briefly, subconfluent hDPSCs at passage 2 were cultured in serum free  $\alpha$ -MEM (Euroclone, Milan, Italy) supplemented with 1 mM  $\beta$ -mercaptoethanol (Sigma Aldrich, Milan, Italy). After 24 h of incubation, the cells were washed in phosphate-buffered saline (PBS) (pH 7.4) and the medium was changed to  $\alpha$ -MEM supplemented with 5% FBS (Euroclone, Milan, Italy) and 35 ng/mL of all-trans-retinoic acid (RA, Sigma Aldrich, Milan, Italy). Following 72 h of incubation, the medium was removed, cells were washed with PBS and replaced in new medium consisting in  $\alpha$ -MEM supplemented with 5% FBS (Euroclone, Milan, Italy), 10 ng/mL basic b-FGF, 5 ng/mL human recombinant platelet derived growth factor (PDGF), 10  $\mu$ M forskolin and 200 ng/ml recombinant human heregulin-b1 (HRG-b1) (Sigma-Aldrich, Milan, Italy). The cells were incubated in this medium for 21 days with media changes every 2–3 days.

At day 21 the concentrations of neurotrophic factors including Brain-Derived Neurotrophic Factor (BDNF), Nerve Growth Factor (NGF) and Neurotrophin 3 (NT-3) were measured in the culture media of undifferentiated hDPSCs and hDPSCs induced towards Schwann cell differentiation. The quantitative measurement of human neurotrophic factors concentration was determined using the Human Multi-Neurotrophin *Rapid*<sup>TM</sup> ELISA kit (Biosensis® Pty Ltd, Thebarton, Australia) according to the manufacturer instruction. Experiments were performed in triplicate and absorbance was measured at 450 nm by means of the Appliskan Multimode Microplate Reader (Thermo Scientific, Waltham, MA USA).

## 2.5 Western blotting

Whole cell lysates were obtained from undifferentiated hDPSCs and hDPSCs differentiated toward Schwann cells at 1, 2 and 3 weeks of differentiation. All cells samples were harvested, washed with PBS, and gently lysed on ice for 10 min in hypotonic lysis buffer (30 mM Tris-HCl, pH 7.8, containing 1% Nonidet P40, 1mM EDTA, 1mM EGTA, 1 mM  $\text{Na}_3\text{VO}_4$ , protease and phosphatase inhibitors cocktail (Sigma Aldrich, Milan, Italy). After brief sonication and micro-centrifugation at 12,000 rpm for 15 minutes at 4°C, the supernatants were collected and the protein concentrations were determined by Bradford (Biorad, Hercules, CA, USA) assay. Forty  $\mu\text{g}$  of total proteins from each sample were separated by 12% sodium dodecyl sulfate-poly acrylamide gel electrophoresis (SDS-PAGE) and then transferred to PVDF membranes. Membranes were incubated overnight at 4°C with mouse anti-P75<sup>NTR</sup> (Biolegend, San Diego, CA, USA), mouse anti-GFAP (Cell Signaling, Danvers, MA, USA), rabbit anti-S100b (Sigma Aldrich, Milan, Italy) primary antibodies (diluted 1:1000 in Tris-buffered saline Tween 20 plus 2% BSA and 3% milk, AbCam, Cambridge, UK). Peroxidase-labeled secondary anti-mouse and anti-rabbit antibodies (Thermo Fisher Scientific, Milan, Italy) were added (diluted 1:3000) for 30 minutes at room temperature. All membranes were visualized using Enhanced Chemio Luminescence (Amersham Biosciences UK Ltd, Buckinghamshire, UK). Goat anti-actin antibody (Santa Cruz Biotechnologies, Dallas, TX, USA) was used as control of protein loading in timing experiments. Densitometry was performed on three independent experiments by ImageJ software. An equal area was selected inside each band and the integrated density was calculated. Data were normalized to values of background and of control actin band.

## 2.6 Animal surgery and cell transplantation

Sprague-Dawley rats aging 12-14 weeks were purchased from Charles River Laboratories (Calco, Lecco, Italy) and were housed under standard condition. Prior to the surgery procedures, rats were anesthetized by ketamine hydrochloride (Ketavet 100®, Farmaceutici Gellini, Milan, Italy) plus xylazine hydrochloride (Rompun®, Bayer AG, Leverkusen, Germany) by intraperitoneal injection. Incision was made along the femoral axis, and thigh muscles were separated apart. Using micro scissors and stereomicroscope the sciatic nerve was exposed, cut along the epineurium and a 6 mm segment containing nerve fibres wrapped by the perineurium and endoneurium was emptied. Immediately thereafter, proximal and distal stumps of sciatic nerve gap were filled by collagen scaffold alone (Type I Collagen, Condress®) or by collagen scaffold injected right after with undifferentiated STRO-1<sup>+</sup>/c-kit<sup>+</sup>/CD34<sup>+</sup> hDPSCs ( $5 \times 10^5$  cells/animal). In order to limit the retraction of the nerve endings, epineurium was sutured with 10-0 resorbable nylon monofilament (Fig. 1). The muscles were then re-apposed with 4-0 vicryl sutures and the skin incision was clamped shut with wound clips. After surgery the rats were placed under warm light, allowed to recover from anaesthesia and then housed separately with access to food and water *ad libitum* in a colony room maintained at constant temperature and humidity on 12:12 hours light/dark cycle. Sham operated (injured untreated) animals not receiving collagen and/or hDPSCs collagen scaffold complex were used as positive controls of sciatic nerve defects. Conversely, animals that did not undergo surgery were used as negative controls. All animals were given cyclosporine A at a dosage of 15 mg/kg body weight, administered 4 hours before transplantation and then daily for 2 weeks as an immunosuppressant to enhance the survival of transplanted cells. During the last week the daily dosage of cyclosporine A was reduced gradually up to 6 mg/kg body weight. Through all the post-operative period the animals were kept monitored to assess any pain or distress following the surgical procedure.

Four weeks after surgical implantation, the rats were sacrificed and sciatic nerves were rapidly explanted and fixed in 4% paraformaldehyde in PBS or 1% glutaraldehyde (Sigma Aldrich, Milan, Italy) for 3 hours. In this study a total of 5-6 animals for each experimental group was used. All animal procedures were performed according to the guidelines approved by the Committee of Use and Care of Laboratory Animals of the University of Modena e Reggio Emilia. All experiments were carried out according to the Bioethical Committee of the Italian National Institute of Health. Animal care, maintenance and surgery were conducted in accordance with Italian Law (D.L. No. 116/1992) and European legislation (86/609/EEC).

## 2.7 Functional analysis

Four weeks post-surgery, the animals underwent paws analysis and measurements of multiple parameters were evaluated: the distance between the first and fifth toes, known as TS, and the distance from the heel to the distal end of the third toe, known as SL. Based on the values of TS and SL, obtained from each experimental group (n=6), the sciatic functional index (SFI), was calculated as follows (de Medinaceli *et al.*, 1982; Bain *et al.*, 1989):

$$SFI = -38.8 [(ESL - NSL)/NSL] + 109.5 [(ETS - NTS)/NTS] + 13.3(EITS - NITS)/NITS] - 8.8$$

A SFI value between 0 and 11% represented normal nerve function, whereas -100% represented complete damage of nerve function, and -11 to -100% incomplete nerve function recovery.

## 2.8 Histological and immunofluorescence analyses

Four weeks after injury, sciatic nerves from the different experimental groups were harvested, fixed in 4% paraformaldehyde, rinsed with PBS, dehydrated with graded ethanol, cleared and embedded in paraffin. Eight  $\mu\text{m}$  thick cross and longitudinal serial sections of the sciatic nerves from each experimental group were obtained. Routine haematoxylin/eosin (H & E) staining was performed in order to analyse morphological details. In order to evaluate the number of regenerated myelinated fibres the samples were processed for epoxy resin embedding as previously described by Gibellini et al. (Gibellini *et al.*, 2012). Particularly semi-thin cross sections obtained from different experimental groups were stained by toluidine blue stain (Sigma Aldrich, Milan, Italy). The total number of myelinated axons was counted from  $\sim 10,000 \mu\text{m}^2$  of the cross-sectional area of the nerve and median area of myelin thickness, median cross-sectional area of myelinated axons, and g-ratio (axonal area/myelinated fiber area) were examined in mid-sections. Counts were carried out on five serial slides per animal ( $n=5$ ) for each experimental group. Data were integrated with confocal analysis. Images of histological samples were obtained with a Nikon Labophot-2 optical microscope equipped with a DS-5Mc CCD colour camera.

Further, histological sections were processed for immunofluorescence labelling, as previously described by Riccio et al. (Riccio *et al.*, 2014). Primary antibodies [rabbit anti-Myelin Protein Zero (MP0, Abcam, Cambridge, UK), mouse anti-neurofilament (NF, Millipore, Darmstadt, Germany), mouse anti-human Nuclei (hNu, Millipore, Darmstadt, Germany) rabbit anti-S100b (Sigma Aldrich, Milan, Italy)] were diluted 1:50 in PBS containing 3% BSA and incubated for 1 hour at room temperature. Secondary antibodies were diluted 1:200 in PBS containing 3% BSA (goat anti-rabbit alexa488, donkey anti-mouse alexa546, goat anti-mouse alexa488 and goat anti-rabbit alexa546, Thermo Fisher Scientific, Milan, Italy) and incubated for 1 hour at room temperature. Negative controls were samples not incubated with the

primary antibody. Nuclei were counterstained with DAPI (Sigma Aldrich, Milan, Italy). The multi-labelling immunofluorescence experiments were carried out avoiding cross-reactions between primary and secondary antibodies.

Fluorescent samples were observed by a Nikon A1 confocal laser scanning microscope. The confocal serial sections were processed with ImageJ software to obtain three-dimensional projections and image rendering was performed by Adobe Photoshop Software.

## **2.9 Data analysis**

Values were reported as mean  $\pm$  SD obtained by groups of 6-7 samples each. Differences between experimental samples were analyzed by ANOVA followed by Newman-Keuls post hoc test. Differences between two groups were analyzed by Student's t-test (GraphPad Prism Software version 5 Inc., San Diego, CA, USA). In any case, significance was set at  $P < 0.05$ .

## **3 Results**

### **3.1 Cell characterization and multipotency evaluation**

The expression of STRO-1, c-Kit and CD34 surface antigens was assayed on hDPSCs expanded *in vitro* before and after the magnetic cell sorting for the three markers by confocal analysis. Particularly, before the immune-selection, about 2% of unsorted hDPSCs was positive for all the three markers. Following the immune-selection, almost all sorted hDPSCs (99%) were simultaneously positive for the three markers. These data confirmed the purity of immune-selected population for the expression of STRO-1, c-Kit and CD34 (Fig. S1A). Moreover, to confirm the stemness of this stem cells population, at passage 1 STRO-1<sup>+</sup>/c-Kit<sup>+</sup>/CD34<sup>+</sup> hDPSCs were differentiated towards osteogenic, myogenic, adipogenic and neurogenic lineages (Fig. S1B). After 4 weeks of osteogenic induction the deposition of mineralized matrix was clearly observed through Alizarin Red staining. The myogenic

commitment of STRO-1<sup>+</sup>/c-Kit<sup>+</sup>/CD34<sup>+</sup> hDPSCs was investigated through immunofluorescence analysis on direct co-culture with C2C12 mouse myoblasts. Analysis revealed that hDPSCs were able to form mature myotubes with murine cells, showing a positivity to myosin heavy chain expression with a direct contribution of hDPSCs, as shown by positive staining for human nuclei. hDPSCs were also able to differentiate toward the adipogenic lineage following 4 weeks of induction. Particularly, lipid rich vacuoles were stained by Oil Red-O. The neurogenic commitment was evaluated by immunofluorescence staining against MAP-2 and TUJ1. Particularly, after 1 week of culture in neurogenic medium hDPSCs started to assume a neuronal-like morphology with multiple cellular processes and a defined cell body. After 2 weeks of induction the co-expression of MAP-2 and TUJ1 was detected, thus confirming the formation of neuron-like cells (Fig. S1B).

### **3.2 Neural crest specific markers evaluation**

At passage 1 immunofluorescence analysis of P75<sup>NTR</sup>, Nestin and Sox-10 was carried out on undifferentiated hDPSCs immune-selected for STRO-1, c-Kit and CD34 and, as shown in the figure 2, a strong expression of the three markers was observed. Moreover, the percentage of cells expressing P75<sup>NTR</sup>, Nestin and Sox-10 was evaluated by means of FACS analysis in three different subjects, demonstrating that almost all the undifferentiated hDPSCs selected for STRO-1 c-Kit and CD34 expressed the three markers (Fig. S2).

### **3.3 Differentiation of hDPSCs towards Schwann cell phenotype and neurotrophins quantification**

Human DPSCs expressing STRO-1, c-Kit and CD34 were induced towards Schwann cells under appropriate conditions and the commitment was evaluated at different time points.

Phase-contrast microscopy revealed that as early as at 1 week of induction, differentiated hDPSCs showed different morphology respect to the original undifferentiated hDPSCs, becoming flattened and showing cell-cell contact. At 2 and 3 weeks of induction respectively, the differentiation became clear through the morphology resembling Schwann cells where differentiated hDPSCs appear elongated bi- or tripolar (Fig. 2A). To evaluate the effective commitment of hDPSCs towards Schwann cells, immunofluorescence analysis was performed against P75<sup>NTR</sup>, GFAP and S100b, all known as markers of Schwann cells. From the analysis of each marker, hDPSCs already expressing P75<sup>NTR</sup> under undifferentiated conditions, showed a higher expression of this marker along the differentiation time. Conversely, undifferentiated hDPSCs did not show any expression of GFAP and S100b which were slightly detectable after 1 week and became more evident after 2 and 3 weeks of induction (Fig. 2A). These data were confirmed by Western blot analysis as shown in figure 3B. Particularly, densitometric analysis revealed that P75<sup>NTR</sup> was already expressed in undifferentiated hDPSCs and gradually increased along the whole differentiation time, reaching a significant value 3 weeks after induction (data not shown). Conversely, the astroglial and/or Schwann cell markers GFAP and S100b were slightly expressed after 1 week of induction, while significant expression was detected only after 2 weeks of differentiation reaching thus a maximum expression at the terminal differentiation stage (3 weeks) when compared with those in the undifferentiated control cells (data not shown). Taken together, these results demonstrated that hDPSCs immune-selected for STRO-1, c-Kit and CD34 have the potential to differentiate into Schwann cells-like cells (Fig. 2B). After 21 days of culture, the quantification of BDNF, NGF and NT-3 was performed in culture media of undifferentiated hDPSCs and hDPSCs induced towards Schwann cell phenotype. Particularly, as reported in figure 2C, low concentrations of BDNF and NGF were detected in undifferentiated hDPSCs media. Following the induction towards Schwann cell phenotype,

high levels of all analyzed trophic factors were observed. Statistically significant values of BDNF and NT-3 ( $***P<0.001$ ) were detected in differentiated hDPSCs. No statistically significant differences were observed between undifferentiated hDPSCs and differentiated hDPSCs media, with regard to NGF secretion.

### **3.4 hDPSCs promote functional recovery of sciatic nerve defects after injury**

In order to evaluate functional recovery, 4 weeks after injury, rats from different experimental groups were kindly placed on transparent plexiglas surfaces and a camera placed below the surface recorded the walking. Subsequently, representative single frames of rat paws from each experimental group were captured, as reported in the figure 3A. For each captured paw frame the TS, SL and SFI were measured. Data from paw analysis revealed a significant greater functional recovery in rats transplanted with hDPSCs-collagen scaffold complex, when compared to both rats transplanted with collagen scaffold alone and untreated injured rats ( $**P<0.01$ ,  $*P<0.05$  vs injured control;  $§§P<0.01$ ,  $§P<0.05$  vs scaffold alone). Significant values of TS, SL and SFI were observed also in uninjured control rats in comparison to untreated injured rats and rats transplanted with collagen scaffold alone (Fig. 3B).

### **3.5. hDPSCs promote regeneration of sciatic nerve defects after injury**

In order to evaluate if the hDPSCs seeded on collagen scaffold were able to restore sciatic nerve defects, *in vivo* implants were performed as described in 2.6 section. Histological analysis revealed that 4 weeks after injury, the injured untreated animals showed a regeneration limited to the proximal stump of nerve gap (Fig. 4B-D). At the same time animals transplanted with collagen scaffold alone showed only a partial and discontinuous regeneration, without any alignment of the regenerating fibres (Fig. 4E, F). Particularly, in

the mid-distal portion the presence of collagen scaffold surrounded by host cells was still detectable showing a reduced and irregular thickness of the whole gap (Fig. 4G). These data suggest that a 6 mm gap in sciatic nerve could not regenerate four weeks after injury, neither when empty nor when filled with the collagen scaffold alone. On the other hand, an appreciable sciatic nerve regeneration from proximal to distal stumps with an aligned arrangement of nerve fibres was observed in animals transplanted with hDPSCs-collagen scaffold complexes (Fig. 4H, 4I). A remodelling process of a few remnants of collagen scaffold by surrounding cells was observed only in the peripheral area of the nerve (Fig. 4J). Moreover, the thickness of the regenerated nerve resembled that of uninjured control (Fig. 4A).

As shown in figure 5, immunofluorescence analysis was carried out on cross-sections of the mid portion of sciatic nerve formerly injured and treated with collagen scaffold alone and with hDPSCs-collagen scaffold complexes, respectively. Confocal analysis revealed a limited and disorganized presence of axons positively stained by anti-MP0 (green) and anti-NF (red) antibodies in the sciatic nerves treated with collagen scaffold alone. Conversely, sciatic nerves treated with hDPSCs-collagen scaffold exhibited NF<sup>+</sup> axons surrounded by myelin (MP0). The distribution of NF<sup>+</sup> MP0<sup>+</sup> axons was spread through the whole section area, resembling the uninjured control. These data were confirmed by toluidine blue stain on semi-thin sections (Fig. 5A). Furthermore, the mid sections of the regenerated sciatic nerves treated with hDPSCs-collagen scaffold contained an average of  $79 \pm 11$  myelinated axons in  $10,000 \mu\text{m}^2$  area compared with  $33 \pm 10$  myelinated axons in  $10,000 \mu\text{m}^2$  area in sciatic nerves treated with collagen scaffold alone, showing a statistically significant difference (\* $P < 0.05$ ) (Fig. 5B). At the same time, the diameter of myelinated axons in the hDPSCs-collagen scaffold group was significantly greater respect to the collagen scaffold group (\*\* $P < 0.01$ ). Similarly, the median myelin thickness in hDPSCs collagen scaffold group was significantly higher

respect to the collagen scaffold group (\* $P < 0.05$ ). No significant difference was observed in the median g-ratios (axonal area/myelinated fiber area) in mid-sections of the nerves in the groups of hDPSCs collagen scaffold complex and collagen scaffold alone ( $0.65 \pm 0.11$  and  $0.75 \pm 0.14$ , respectively) (Fig. 5B).

### **3.6 Sciatic nerve regeneration, arrangement of new myelinated fibres and engraftment of hDPSCs into microenvironment**

Immunofluorescence labelling was performed on longitudinal serial sections of sciatic nerve from the different experimental groups (Fig. 6). Four weeks after surgery, we observed an incomplete and/or minimal sciatic nerve regeneration in the animals formerly injured and treated with collagen scaffold alone. Particularly as shown in figure 6Aii, we observed the presence of fibres positively stained for MP0 (green) and NF (red) at the proximal stumps. Although myelinated axons were visible, the distribution of the fibres was irregular and the stain for both markers (NF and MP0) was slight. Analyzing the distal stumps, the presence of myelinated axons appeared reduced and nerve gaps were observed; the few fibres positively stained for MP0 and NF were distributed in a non-arranged manner. On the other hand, a more complete sciatic nerve regeneration from the proximal to distal stumps was observed 4 weeks after injury in the hDPSCs-collagen scaffold complexes treated group with respect to the group treated with collagen scaffold alone. Particularly, at the proximal stump, the presence of oriented/aligned myelinated fibres (positive for NF and MP0) was detected. Furthermore, at the distal stump, the fibres positively stained for NF and MP0 were spread in a non-arranged manner (Fig. 6Aiii). In order to evaluate the contribution of hDPSCs-collagen scaffold complex to integrate in the host sciatic nerve, immunofluorescence analysis was performed in longitudinal serial sections against human Nuclei (hNu) and S100b. As shown in Figure 6B some of the donor cells, positive for hNu (green) integrated in the host

regenerating nerve and exhibited the expression of S100b (red) (Fig. 6B, white arrows). These data demonstrated that hDPSCs were able to survive, engraft and express *in vivo* Schwann cells markers.

#### 4. Discussion

In the present study, we evaluated the ability of hDPSCs to differentiate into cells with Schwann cell phenotype *in vitro* and their potential to integrate and support the regeneration of peripheral nerve injuries. Although many researchers demonstrated the ability of mesenchymal stem cells isolated from different sources (Mimura *et al.*, 2004; Liu *et al.*, 2011; Pan *et al.*, 2006; Ribeiro *et al.*, 2013; Ren *et al.*, 2012) to differentiate towards SCs and enhance regeneration in injured sciatic nerve, only a few reports demonstrated the ability of human dental pulp stem cells to be committed toward Schwann cells (Martens *et al.*, 2014; Al-Zer *et al.*, 2015). It is well established that the use of mesenchymal stem cells in cell therapy approaches to generate various types of neurons and glia represents a valid tool for nerve injuries repair. Considering the shared embryological derivation of SCs and hDPSCs from neural crest, these stem cells could represent an attractive cell source. In addition to this neural crest origin, the isolation and characterization of hDPSCs subpopulation strictly derived from neuro-ectoderm might provide an excellent candidate for regenerative medicine purposes especially in the field of neural tissue engineering. In this study, we used the hDPSCs subpopulation expressing specific markers: STRO-1, c-Kit and CD34. In accordance with previous reports (Laino *et al.*, 2005; Laino *et al.*, 2006; Pisciotto *et al.*, 2015a) this subpopulation could represent the stem cell niche directly correlated to neural crest migrating cells entrapped within human dental pulp. In support of this statement, our results demonstrated and confirmed that almost all STRO-1<sup>+</sup>/c-Kit<sup>+</sup>/CD34<sup>+</sup> hDPSCs express P75<sup>NTR</sup>, Nestin and Sox-10. Interestingly, it has been well established during craniofacial

development that neural crest cells migrate to branchial arches and contribute extensively to the formation of mesenchymal structures in the head and neck including the tooth. After migration, neural crest cells are able to commit towards different cell types including mesenchyme and neuro-ectoderm derived lineages, thus allowing to define them as neuroecto-mesenchyme derived cells (Noden, 1991; Imai *et al.*, 1996). In accordance with the state of the art, our findings demonstrated that this hDPSCs subpopulation expressing STRO-1, c-Kit and CD34 is able to differentiate towards osteogenic, adipogenic, myogenic and neurogenic lineages. Moreover, we have previously reported (Pisciotta *et al.*, 2015a) that only this niche showed the ability to differentiate toward the neurogenic commitment. Based on these reports, the goal of our study was to investigate the ability of this hDPSCs subpopulation to commit towards Schwann cells after incubation in appropriate induction media at different time points. Following the *in vitro* induction under controlled conditions, differentiated hDPSCs assumed a different morphology as early as after 1 week of culture, becoming clearly bi- and tripolar shaped, resembling SCs, at 3 weeks of induction as widely reported by Jessen and Mirsky (Jessen and Mirsky, 1999). Together with a change in morphology an increase of P75<sup>NTR</sup> expression was observed while GFAP and S100b started to be expressed after 1 week, becoming strongly detectable along the culture time. This early expression of Schwann cell markers might confirm a predisposition of STRO-1<sup>+</sup>/c-Kit<sup>+</sup>/CD34<sup>+</sup> hDPSCs to the glial commitment. These data, in accordance to other reports, strengthen the evidence that this niche could be closely derived from neural crest. The model of sciatic nerve injury is the most commonly used in evaluating peripheral nerve injury and the subsequent integration/regeneration, following the graft with stem cells-scaffold complexes. The conventional approaches consist of injuries caused by resection of short or long segment of nerve, which commonly result in spontaneous regeneration although with a poor functional recovery attributed to the retraction of the nerve during the recovery period

(Rosen *et al.*, 1989; Lundborg *et al.*, 1982; Scherman *et al.*, 2000). In consideration of findings from Isaacs *et al.* (Isaacs *et al.*, 2014), we designed a specific method aimed to limit the gap oversizing, due to nerve endings retraction, and the collapse of stem cells-scaffold complex. This surgical approach ensured that the healing of nerve injury was not due to spontaneous regeneration by the host. Indeed, we observed a minimal regeneration limited to the proximal stump when the gap was not filled with any construct. In our *in vivo* study, the graft of hDPSCs-collagen scaffold complex integrated into the sciatic nerve defect in rats, promoting nerve fibres regeneration and myelination, as revealed by histological and confocal analyses. Despite of the limited experimental recovering time (1 month) we observed a significant number of myelinated axons particularly in the mid-portion associated to the restored nerve diameter and a minimal presence of collagen remnants. Our findings demonstrated the presence of myelinated fibres densely spread and aligned as much as possible regularly along the entire gap, from proximal to distal stumps. The presence of hDPSCs positively labelled by anti-hNu antibody indicates that these cells survived, integrated in host tissue and contributed to regeneration of axons promoting myelination. In support of these results, human DPSCs (hNu<sup>+</sup> cells) positively labelled against S100b were detected in the regenerated portion of the nerve 1 month after the treatment. Based on these results, we can conclude that hDPSCs directly contributed to axonal regeneration and myelination, event that was not observed in the animal group treated with the collagen scaffold alone. However, although there was a clear hDPSCs engraftment, given their low number compared to host cells, the histological improvement previously described, might not be closely due to terminal differentiation of hDPSCs. Moreover, as demonstrated hDPSCs are able to produce in vitro neurotrophic factor such as BDNF, NGF and NT-3. This is in accordance with previous findings by Martens *et al.*, Sasaki *et al.* and by de Almeida *et al.* (Martens *et al.*, 2014; Sasaki *et al.*, 2008; de Almeida *et al.*, 2011), although they used the

whole cell population derived from dental pulp. Particularly, we observed a statistically significant increase of BDNF and NT-3 at three weeks of induction. This is in compliance with previous data by Jessen and Mirsky and by Ma et al. (Jessen and Mirksy, 1999; Ma *et al.*, 2011), who demonstrated that Schwann cells precursors can survive in absence of axons, due to autocrine secretion of neurotrophic factors, such as NT-3, and can differentiate, following the secretion of BDNF. To this regard it may be argued that hDPSCs exert their regenerative function at least in part via paracrine mechanisms that promote changes in host cells activity, as demonstrated by several findings on different stem cell types (Gharaibeh *et al.*, 2011). Therefore, mechanisms observed here that may contribute to the nerve healing include the recruitment of host cells to the site of injury, then proliferation, and differentiation of host cells toward a supporting cell lineage, such as Schwann cells, which release cytokines that exert neuroprotective effects independently of neurogenesis (Maiese *et al.*, 1993; Nozaki *et al.*, 1993). Moreover, as previously demonstrated by Martens et al. (Martens *et al.*, 2014), hDPSCs differentiated into SCs are able to provide a strong guidance cue *in vitro* to neurite growth, by providing the alignment of nerve fibres and by secreting neurotrophins, processes that are necessary to promote neural regeneration *in vivo*. Taken together these data suggest that STRO-1<sup>+</sup>/c-Kit<sup>+</sup>/CD34<sup>+</sup> hDPSCs might contribute in promoting peripheral nerve regeneration. In association with histological evaluation, we demonstrated that animals treated with hDPSCs-collagen scaffold complexes took advantage of functional recovery. In conclusion, this study demonstrates that STRO-1<sup>+</sup>/c-Kit<sup>+</sup>/CD34<sup>+</sup> hDPSCs, a cellular niche associated to neural crest derivation, could represent a challenging source of stem cells for the treatment of demyelinating disorders. Although further investigations are needed, the use of this hDPSCs subpopulation could provide a feasible source of cells and a valid alternative tool for future clinical applications aimed to achieve functional recovery after injury or peripheral neuropathies.

**Financial support:** This work was supported by grants from “Progetto Strategico per lo sviluppo nella sede di Reggio Emilia della Facoltà di Medicina e Chirurgia” Prot: 2010 0007725, Arcispedale S. Maria Nuova di Reggio Emilia and MIUR FIRB Accordi di Programma 2010 Prot: RBAP10Z7FS

**Disclosures:** The authors declare no competing financial interests.

## References

- Aguayo AJ, Kasarjian J, Skamene E, et al. 1977. Myelination of mouse axons by Schwann cells transplanted from normal and abnormal human nerves. *Nature* 268, 753-755.
- Al-Zer H, Apel C, Heiland M, et al. 2015. Enrichment and Schwann Cell Differentiation of Neural Crest-derived Dental Pulp Stem Cells. *In Vivo* 29, 319-326.
- Ansselin AD, Fink T, Davey DF. 1997. Peripheral nerve regeneration through nerve guides seeded with adult Schwann cells. *Neuro. Pathol. Appl. Neurobiol.* 23, 387-398.
- Arthur A, Rychkov G, Shi S, et al. 2008. Adult human dental pulp stem cells differentiate toward functionally active neurons under appropriate environmental cues. *Stem Cells* 26, 1787–1795.
- Bain JR, Mackinnon SE, Hunter DA. 1989. Functional evaluation of complete sciatic, peroneal, and posterior tibial nerve lesions in the rat. *Plast. Reconstr. Surg.* 83, 129-138.
- Calderón-Martínez D, Garavito Z, Spinel C, et al. 2002. Schwann cell-enriched cultures from adult human peripheral nerve: a technique combining short enzymatic dissociation and treatment with cytosine arabinoside (Ara-C). *J. Neurosci. Methods* 114, 1-8.
- Carnevale G, Riccio M, Pisciotta A, et al. 2013. In vitro differentiation into insulin-producing  $\beta$ -cells of stem cells isolated from human amniotic fluid and dental pulp. *Dig. Liver Dis.* 45, 669-676.
- Caton J, Tucker AS. 2009. Current knowledge of tooth development: patterning and mineralization of the murine dentition. *J. Anat.* 214, 502–515.
- Chai Y, Jiang X, Ito Y, et al. 2000. Fate of the mammalian cranial neural crest during tooth and mandibular morphogenesis. *Development* 127, 1671–1679.

Chernousov MA, Carey DJ. 2000. Schwann cell extracellular matrix molecules and their receptors. *Histol. Histopathol.* 15, 593-601.

de Almeida FM, Marques SA, Ramalho Bdos S, et al. 2011. Human dental pulp cells: a new source of cell therapy in a mouse model of compressive spinal cord injury. *J Neurotrauma.* 28, 1939-1949.

de Medinaceli L, Freed WJ, Wyatt RJ. 1982. An index of the functional condition of rat sciatic nerve based on measurements made from walking tracks. *Exp. Neurol.* 77, 634-643.

Deng W, Obrocka M, Fischer I, et al. 2001. In vitro differentiation of human marrow stromal cells into early progenitors of neural cells by conditions that increase intracellular cyclic AMP. *Biochem. Biophys. Res. Commun.* 282, 148–152.

Dezawa M, Takahashi I, Esaki M, et al. 2001. Sciatic nerve regeneration in rats induced by transplantation of in vitro differentiated bone-marrow stromal cells. *Eur. J. Neurosci.* 14, 1771-1776.

Fu SY, Gordon T. 1997. The cellular and molecular basis of peripheral nerve regeneration. *Mol. Neurobiol.* 14, 67-116.

Gharaibeh B, Lavasani M, Cummins JH, et al. 2011. Terminal differentiation is not a major determinant for the success of stem cell therapy - cross-talk between muscle-derived stem cells and host cells. *Stem Cell Res. Ther.* 2, 31.

Gibellini L, De Biasi S, Pinti M, et al. 2012. The protease inhibitor atazanavir triggers autophagy and mitophagy in human preadipocytes. *AIDS* 26, 2017-2026.

Goldberg JL, Barres BA. 2000. The relationship between neuronal survival and regeneration. *Annu. Rev. Neurosci.* 23, 579-612.

Graham A, Begbie J, McGonnell I. 2004. Significance of the cranial neural crest. *Dev. Dyn.* 229, 5–13.

Gronthos S, Brahimi J, Li W, et al. 2002. Stem cell properties of human dental pulp stem cells. *J. Dental Res.* 81, 531–535.

Hill CE, Moon LD, Wood PM, et al. 2006. Labeled Schwann cell transplantation: cell loss, host Schwann cell replacement, and strategies to enhance survival. *Glia* 53, 338–343.

Ibarretxe G, Crende O, Aurrekoetxea M, et al. 2012. Neural crest stem cells from dental tissues: a new hope for dental and neural regeneration. *Stem Cells Int.* 2012, 103503.

Imai H, Osumi-Yamashita N, Ninomiya Y, et al. 1996. Contribution of early-emigrating midbrain crest cells to the dental mesenchyme of mandibular molar teeth in rat embryos. *Dev. Biol.* 176, 151-165.

Isaacs J, Mallu S, Yan W, et al. 2014. Consequences of oversizing: nerve-to-nerve tube diameter mismatch. *J. Bone Joint Surg. Am.* 96, 1461-1467.

Iwashita Y, Fawcett JW, Crang AJ, et al. 2000. Schwann cells transplanted into normal and X-irradiated adult white matter do not migrate extensively and show poor long-term survival. *Exp. Neurol.* 164, 292–302.

Jessen KR, Mirsky R. 2005. The origin and development of glial cells in peripheral nerves. *Nat. Rev. Neurosci.* 6, 671-682.

Jessen KR, Mirsky R. 1999. Why do Schwann cells survive in the absence of axons? *Ann N Y Acad Sci.* 14, 109-115.

Kiraly M, Porcsalmy B, Pataki A, et al. 2009. Simultaneous PKC and cAMP activation induces differentiation of human dental pulp stem cells into functionally active neurons. *Neurochem. Int.* 55, 323–332.

Laino G, d'Aquino R, Graziano A, et al. 2005. A new population of human adult dental pulp stem cells: a useful source of living autologous fibrous bone tissue (LAB). *J. Bone Miner. Res.* 8, 1394–1402.

Laino G, Graziano A, d'Aquino R, et al. 2006. An approachable human adult stem cell source for hard-tissue engineering. *J. Cell Physiol.* 206, 693-701.

Liu GB, Cheng YX, Feng YK, et al. 2011. Adipose-derived stem cells promote peripheral nerve repair. *Arch. Med. Sci.* 7, 592-596.

Lundborg G, Dahlin LB, Danielsen N, et al. 1982. Nerve regeneration across an extended gap: a neurobiological view of nerve repair and the possible involvement of neuronotrophic factors. *J. Hand Surg. Am.* 7, 580-587.

Ma Z, Wang J, Song F, et al. 2011. Critical period of axoglial signaling between neuregulin-1 and brain-derived neurotrophic factor required for early Schwann cell survival and differentiation. *J Neurosci.* 31, 9630-9640

Maiese K, Boniece I, De Meo D, et al. 1993. Peptide growth factors protect against ischemia in culture by preventing nitric oxide toxicity. *J. Neurosci.* 13, 3034–3040.

Martens W, Bronckaers A, Politis C, et al. 2013. Dental stem cells and their promising role in neural regeneration: an update. *Clin. Oral Invest.* 17, 1969–1983.

Martens W, Sanen K, Georgiou M, et al. 2014. Human dental pulp stem cells can differentiate into Schwann cells and promote and guide neurite outgrowth in an aligned tissue-engineered collagen construct in vitro. *FASEB J.* 4, 1634-1643.

Miletich I, Sharpe PT. 2004. Neural crest contribution to mammalian tooth formation. *Birth Defect Res.*72, 200–212.

Mimura T, Dezawa M, Kanno H, et al. 2004. Peripheral nerve regeneration by transplantation of bone marrow stromal cell-derived Schwann cells in adult rats. *J. Neurosurg.* 101, 806-812.

Morrissey TK, Kleitman N, Bunge RP. 1991. Isolation and functional characterization of Schwann cells derived from adult peripheral nerve. *J. Neurosci.*11, 2433-2442.

Mosahebi A, Woodward B, Wiberg M, et al. 2001. Retroviral labeling of Schwann cells: in vitro characterization and in vivo transplantation to improve peripheral nerve regeneration. *Glia* 34, 8-17.

Noden DM. 1991. Cell movements and control of patterned tissue assembly during craniofacial development. *J. Craniofac. Genet. Dev. Biol.* 11, 192-213.

Nozaki K, Finklestein SP, Beal MF. 1993. Basic fibroblast growth factor protects against hypoxia-ischemia and NMDA neurotoxicity in neonatal rats. *J. Cereb. Blood Flow Metab.* 13, 221–228.

Pan HC, Yang DY, Chiu YT, et al. 2006. Enhanced regeneration in injured sciatic nerve by human amniotic mesenchymal stem cell. *J. Clin. Neurosci.*13, 570-575.

Pisciotta A, Carnevale G, Meloni S, et al. 2015a. Human Dental pulp stem cells (hDPSCs): isolation, enrichment and comparative differentiation of two sub-populations. *BMC Dev. Biol.* 15, 14.

Pisciotta A, Riccio M, Carnevale G, et al. 2012. Human serum promotes osteogenic differentiation of human dental pulp stem cells in vitro and in vivo. *PLoS One* 7, e50542.

Pisciotta A, Riccio M, Carnevale G, et al. 2015b. Stem cells isolated from human dental pulp and amniotic fluid improve skeletal muscle histopathology in mdx/SCID mice. *Stem Cell Res Ther.* 28,6:156.

Ren Z, Wang Y, Peng J, et al. 2012. Role of stem cells in the regeneration and repair of peripheral nerves. *Rev. Neurosci.* 23, 135-143.

Ribeiro J, Gartner A, Pereira T, et al. 2013. Perspectives of employing mesenchymal stem cells from the Wharton's jelly of the umbilical cord for peripheral nerve repair. *Int. Rev. Neurobiol.* 108, 79-81.

Riccio M, Carnevale G, Cardinale V, et al. 2014. The Fas/Fas ligand apoptosis pathway underlies immunomodulatory properties of human biliary tree stem/progenitor cells. *J. Hepatol.* 61, 1097-1105.

Rosen JM, Pham HN, Hentz VR. 1989. Fascicular tubulization: a comparison of experimental nerve repair techniques in the cat. *Ann. Plast. Surg.* 22, 467-478.

Sasaki R, Aoki S, Yamato M, et al. 2008. Tubulation with dental pulp cells promotes facial nerve regeneration in rats. *Tissue Eng Part A* 14, 1141-1147.

Scherman P, Lundborg G, Kanje M, et al. 2000. Sutures alone are sufficient to support regeneration across a gap in the continuity of the sciatic nerve in rats. *Scand. J. Plast. Reconstr. Surg. Hand Surg.* 34, 1-8.

Sofroniew MV, Howe CL, Mobley WC. 2001. Nerve growth factor signaling, neuroprotection, and neural repair. *Annu. Rev. Neurosci.* 24:1217-81.

Thesleff I, Aberg T. 1999. Molecular regulation of tooth development. *Bone* 25, 123–125.

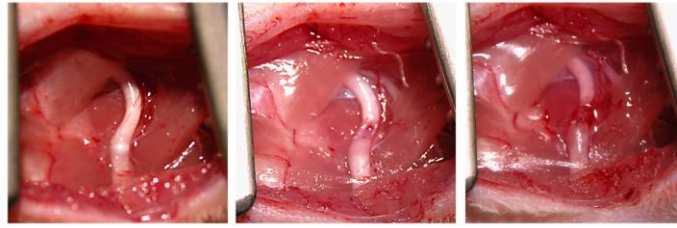


**Figure 1. Surgical procedures**

*Left:* uninjured control of rat sciatic nerve (before surgery); *middle:* surgically-operated sciatic nerve gap; *right:* sciatic nerve gap filled by hDPSCs/collagen scaffold or collagen scaffold alone.

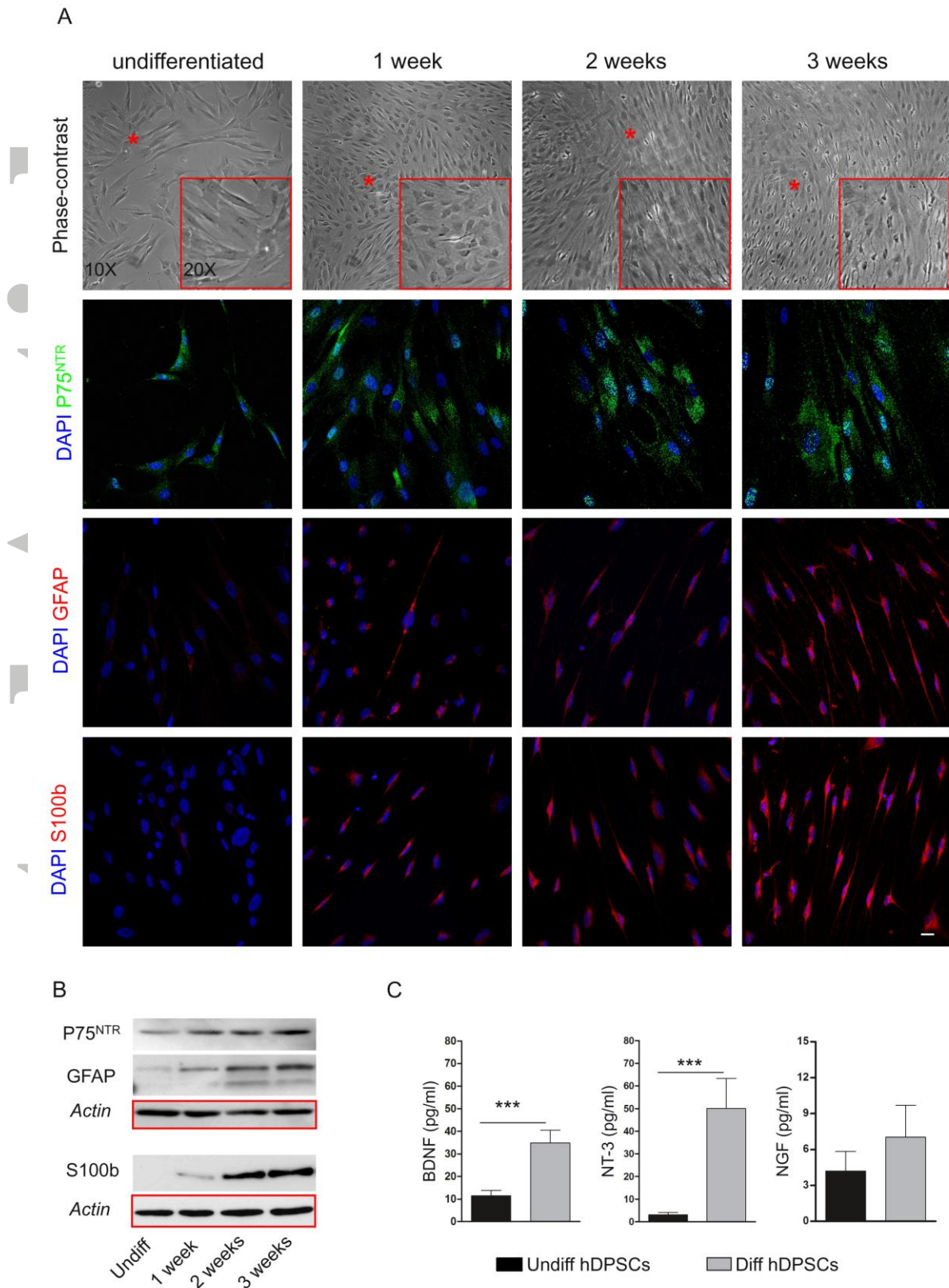


**Figure 2. Differentiation of hDPSCs towards Schwann cells-like cells.** A) Phase contrast images of undifferentiated hDPSCs and hDPSCs following induction towards Schwann cells

Accepted Article

at different time points. Red asterisks refer to higher magnification inset enclosed at the lower right corner of each image. Confocal analysis of undifferentiated hDPSCs and differentiated hDPSCs at different time points, labelled by: DAPI/anti-P75<sup>NTR</sup>, DAPI/anti-GFAP, and DAPI/anti-S100b, as indicated. Bar = 10  $\mu$ m. **B)** WB analysis of P75<sup>NTR</sup>, GFAP and S100b expression in whole cell lysates from undifferentiated hDPSCs, and from differentiated hDPSCs at different time points. Actin bands were presented as control of the protein loading. **C)** Histograms represent concentrations of BDNF, NT-3 and NGF, expressed as mean  $\pm$  SD following ELISA analysis. \* Indicates significant values of Student's t-test of differentiated hDPSCs vs. undifferentiated hDPSCs (\*\*\*P <0.001).

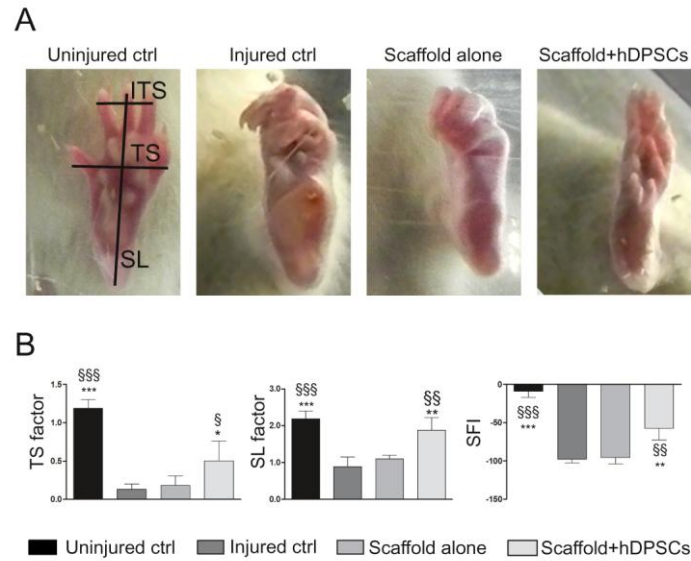


**Figure 3. Functional recovery.** **A)** Representative single frames of rats paws from each experimental group, 4 weeks after injury. **B)** Histograms represent the values of TS, SL and SFI. Values were expressed as mean  $\pm$  SD of five animals for each experimental group and statistical analysis was performed by ANOVA followed by Newman-Keuls post-hoc test: \*\*\* $P < 0.001$ , \*\* $P < 0.01$ , \* $P < 0.05$  vs injured control; §§§ $P < 0.001$ , §§ $P < 0.01$ , § $P < 0.05$  vs scaffold alone.

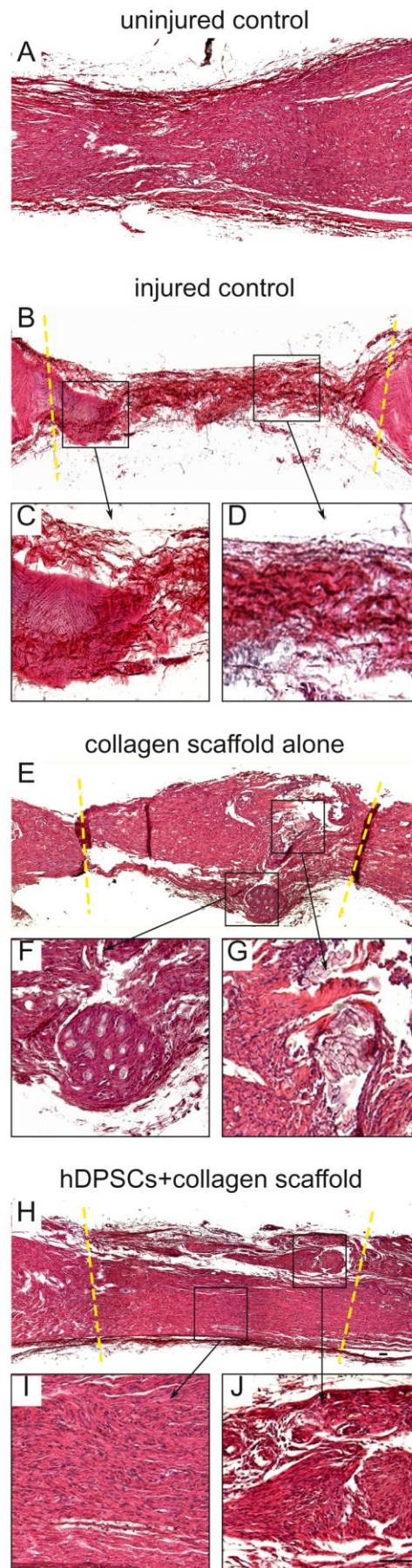


**Figure 4. Comparative histological analysis of the sciatic nerve defects 30 days post-injury.** Representative images show longitudinal sections obtained through the whole area of the implants. A) Uninjured control sciatic nerve experimental group; B-D) injured untreated sciatic nerve experimental group. E-G) sciatic nerve injury filled by collagen scaffold alone. H-J) sciatic nerve injury filled by hDPSCs-collagen scaffold implant. Bar = 100  $\mu$ m.

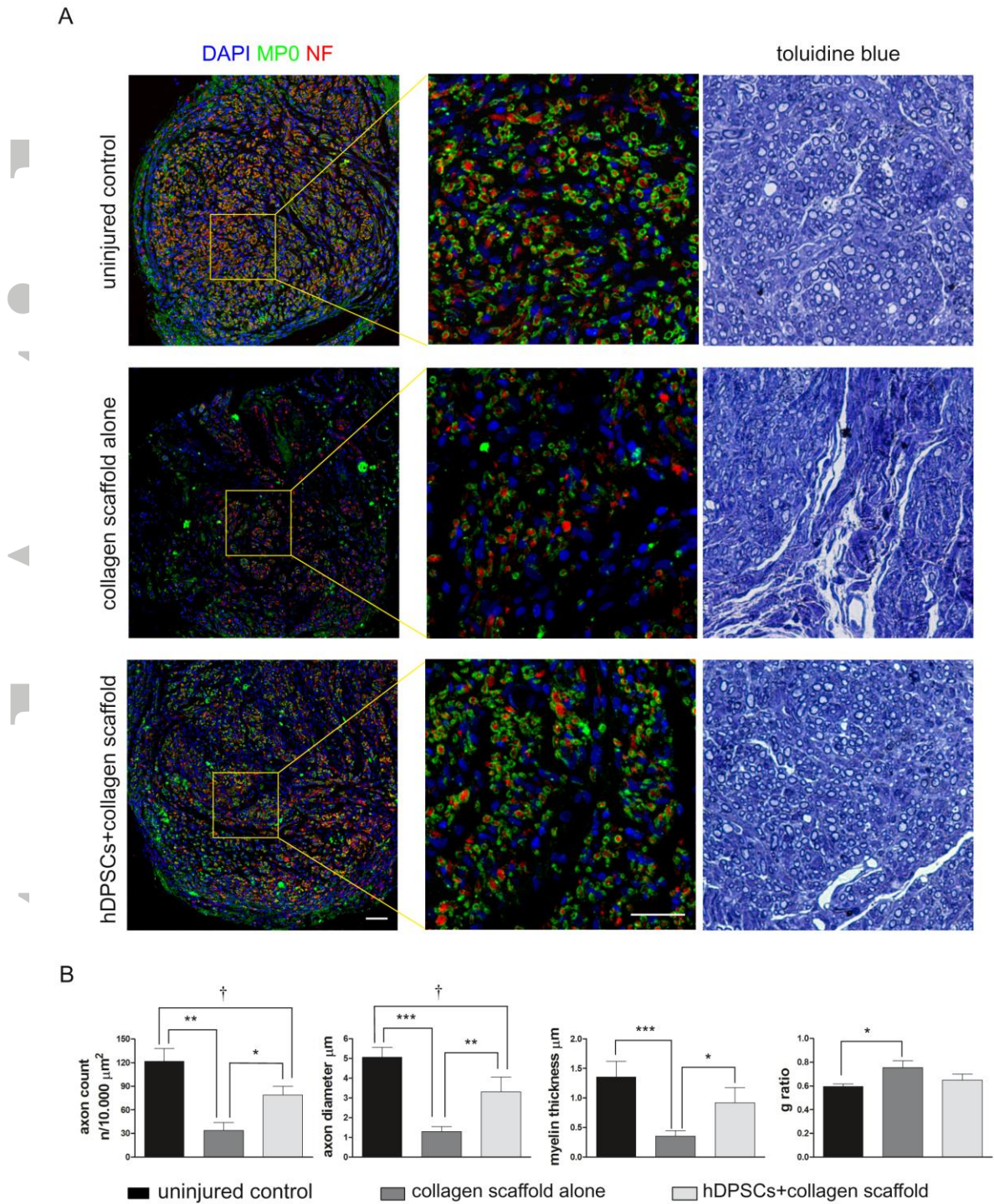


**Figure 5. Comparative confocal analysis of sciatic nerve regeneration after injury. A)**

Representative immunofluorescence images taken on cross-sections of the mid-portion of sciatic nerve formerly injured and treated with collagen scaffold alone, with hDPSCs-collagen scaffold complexes and compared to uninjured control, as indicated.

Immunostaining was performed against Myelin Protein Zero (MP0, green) and Neurofilament (NF, red). DAPI staining was shown in blue. Toluidine blue stain was carried out on semi-thin sections and reported at the far end of each experimental group. Bar=50  $\mu\text{m}$ .

**B)** Histograms represent the number of myelinated axons counted on areas of 10,000  $\mu\text{m}^2$ , axon diameter, myelin thickness and g-ratio, for each experimental group. Values were expressed as mean  $\pm$  SD of five different slides from five animals for each experimental group. \*\*\* $P < 0.001$ , \*\* $P < 0.01$ , \* $P < 0.05$  indicates significant values of ANOVA followed by Newman-Keuls post-hoc test of uninjured control and hDPSCs collagen scaffold complex vs collagen scaffold alone. <sup>†</sup> $P < 0.05$  uninjured control vs hDPSCs collagen scaffold complex.

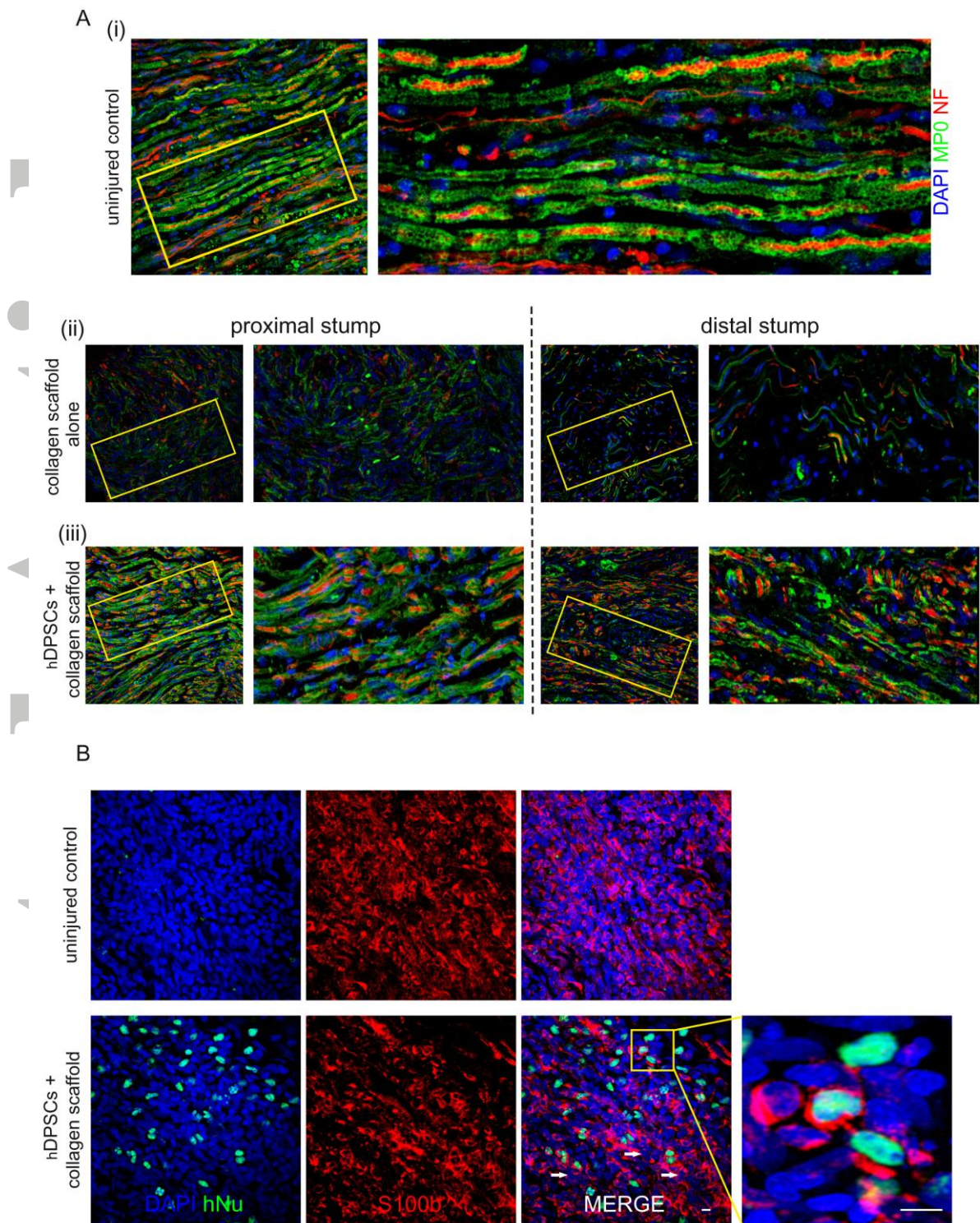


**Figure 6. Sciatic nerve regeneration, arrangement of new myelinated fibres and engraftment of hDPSCs into microenvironment.** A) Representative immunofluorescence images taken on longitudinal nerve sections from uninjured control group and with collagen scaffold alone and from sciatic nerve defects filled with hDPSCs-collagen scaffold

complexes (i). Low- and High- magnification images show immunostaining for Myelin (MP0, green) and Neurofilament (NF, Red) from proximal to distal stumps of sciatic nerve defects following implants with collagen scaffold alone (ii) and with hDPSCs-collagen scaffold complex (iii). DAPI staining was shown in blue.

**B)** Representative images of immunostained longitudinal sections of regenerating sciatic nerve show the engraftment of hNu<sup>+</sup> hDPSCs (green) and the expression of Schwann cell marker S100b (Red). White arrows indicate the presence of human cells expressing S100b. Nuclei were counterstained by DAPI (blue). Immunostained longitudinal sections of uninjured control were taken as negative control of anti-hNu staining. Bar = 10μm.